

Translocation *versus* cyclisation in radicals derived from *N*-3-alkenyl trichloroacetamidesM. Luisa Marin,^{a*} Ramon J. Zaragoza,^{*b} Miguel A. Miranda,^a Faïza Diaba^c and Josep Bonjoch^c

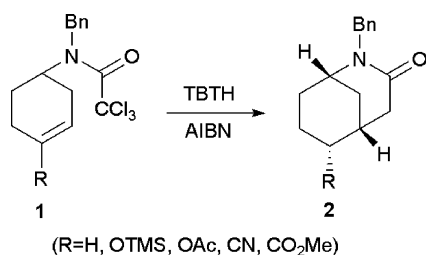
Received 21st December 2010, Accepted 17th February 2011

DOI: 10.1039/c0ob01228a

Under radical reaction conditions, two different and competitive reaction pathways were observed for *N*-(α -methylbenzyl)trichloroacetamides with a *N*-3-cyclohexenyl substituent: 1,4-hydrogen translocation and radical addition to a double bond. However, for radicals with an acyclic alkenyl side chain, the direct cyclisation process was exclusively observed. The dichotomy between translocation and direct radical cyclisation in these substrates has been theoretically studied using density functional theory (DFT) methods at the B3LYP/6-31G** computational level.

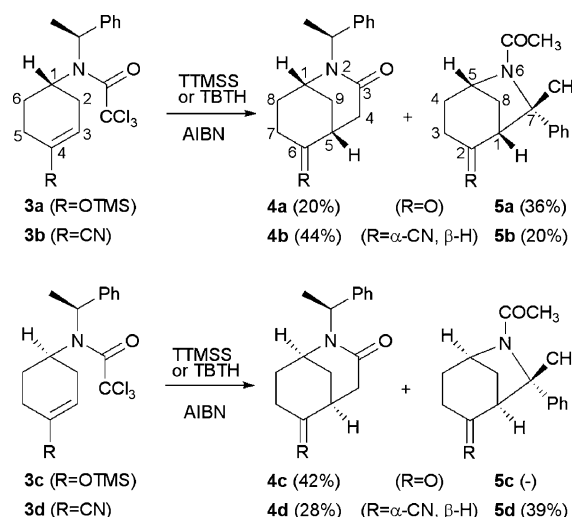
Introduction

Trichloroacetamides have been used since the 1980s as radical precursors to synthesise nitrogen-containing heterocycles, such as β -, γ -, and δ -lactams, in a variety of radical processes (e.g. atom transfer mediated by CuCl¹ or Grubbs' ruthenium metathesis catalysis,² and the hydride reductive method³). Their usefulness in radical cyclisations leading to 6-membered rings can be attributed to the stability of the formed *N*-(3-alkenyl)carbamoyldichloromethyl radicals, which reduces the occurrence of the disruptive 1,5-hydrogen shift.⁴ Several years ago, we showed that *N*-benzyl-*N*-cyclohexenyl trichloroacetamides **1** are versatile reagents for the synthesis of 2-azabicyclo[3.3.1]nonanes **2** (Scheme 1), *via* radical cyclisation.⁵



Scheme 1 Synthesis of 2-azabicyclo[3.3.1]nonanes.

Attempts to extend this morphan approach to the synthesis of enantiopure compounds with a (*S*)-1-phenylethyl group at the nitrogen produced a surprising result when using either electron-rich⁶ or electron-poor⁷ radical acceptors (Scheme 2). Together

Scheme 2 The synthesis of 2-azabicyclo[3.3.1]nonanes (**4**) together with normorphans (**5**) from electron-rich (**3a** and **3c**) or electron-poor (**3b** and **3d**) *N*-cyclohexenyl trichloroacetamides.

with the expected 2-azabicyclo[3.3.1]nonanes **4**, the normorphans **5** were also isolated. The former are the result of 6-*exo*-trig radical cyclisation, whereas the latter arise from a competitive process involving 1,4-hydrogen transfer,⁸ followed by 5-*exo*-trig cyclisation with configurational inversion at the stereogenic benzylic carbon.

At this point, we decided to explore the scope of this unprecedented radical rearrangement occurring in the tin hydride-promoted cyclisation of trichloroacetamides bearing a *N*-(1-phenylethyl) substituent.⁹ To assess whether translocation is a process particular to the synthesis of morphans or whether it can also occur when other alkylbenzyl moieties are present, simple open-chain trichloroacetamides (**6**, **7**, and **9**) were prepared, and their behaviour under radical reaction conditions (using the hydride method) was examined.

^aInstituto de Tecnología Química-Departamento de Química (UPV-CSIC), Avda de los Naranjos s/n, E-46022, Valencia, Spain. E-mail: marmarin@qim.upv.es; Fax: + 34963877809; Tel: + 34963877815

^bDepartamento de Química Orgánica, Universidad de Valencia, Dr Moliner 50, 46100, Burjassot, Valencia, Spain. E-mail: ramon.j.zaragoza@uv.es

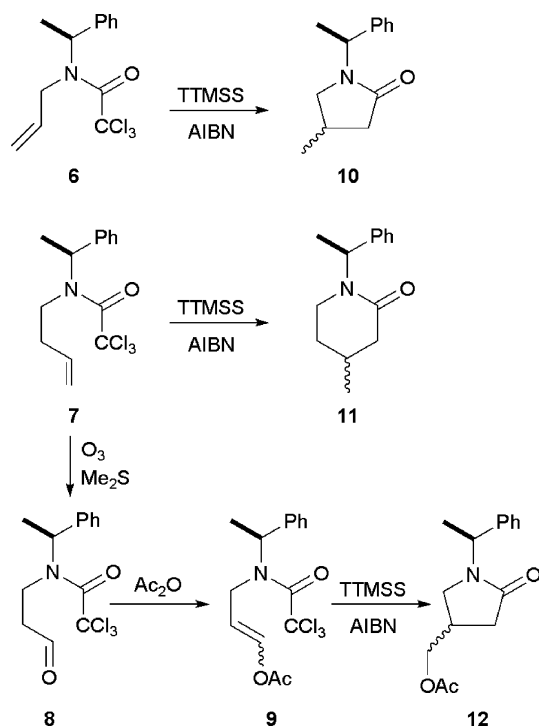
^cLaboratori de Química Orgànica, Facultat de Farmàcia, Institut de Biomedicina (IBUB), Universitat de Barcelona, Av., Joan XXIII s/n, 08028-, Barcelona, Spain

To obtain further insight into these radical processes leading to mono- and bicyclic compounds, theoretical studies on their reaction pathways were also carried out. Thus, the reductive cyclisation of trichloroacetamides **7**, **3b**, **1** ($R=CN$) and **3d** has been studied by means of DFT calculations. Based on the theoretical data obtained, different reaction mechanisms are proposed to explain the experimental results.

Results and discussion

Synthetic studies

Preparation of the starting materials **6** and **7** from the corresponding amines in the trichloroacetylation step was improved from the previously reported procedure.¹⁰ The unreported trichloroacetamide **9** was prepared from **7** by ozonolysis to give aldehyde **8**, followed by treatment with isopropenyl acetate.¹¹ The enol acetate **9** was obtained as a mixture of *Z/E* isomers (4 : 6 ratio) (Scheme 3). When trichloroacetamides **6**, **7** and **9** were treated with tris(trimethylsilyl)silane (TTMSS)/AIBN, pyrrolidone **10** (80%) and piperidones **11** (53%) and **12** (78%) were, respectively, formed. The isolated compounds are the result of cyclisation of the 1-(carbamoyl)dichloromethyl radical onto the double bond without any diastereoselectivity (epimeric 1:1 mixtures were obtained in every case). The 1,4-translocation products were not detected for these open-chain trichloroacetamides that contain the alkylbenzyl moiety but lack the cyclohexene. Therefore, it seems that both structural features are required to observe the translocation process.



Scheme 3 Cyclisation of trichloroacetamides **6**, **7** and **9**.

Theoretical DFT studies

i) Conversion of **7 into **11** and **11a**.** The suggested mechanism is depicted in Scheme 4; the energies of the relevant species are

Table 1 Total (*E*, au) and relative energies (ΔE , kcal mol⁻¹), at the B3LYP/6-31G** level in benzene, of the stationary points for the radical transformations of **7** leading to **11** and **11a**

	<i>E</i>	ΔE
R-1	-1593.447221	0.0
TS1-si	-1593.425862	13.4
TS1-re	-1593.426832	12.8
R-2-si	-1593.464250	-10.7
R-2-re	-1593.466231	-11.9
TS2	-1593.424075	14.5
R-3	-1593.462295	-9.5
TS3-si	-1593.432970	8.9
TS3-re	-1593.437124	6.3
R-4-si	-1593.453740	-4.1
R-4-re	-1593.457743	-6.6

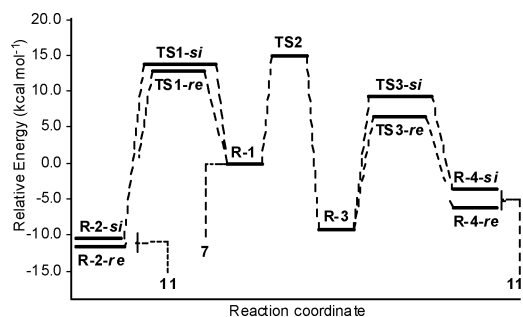


Fig. 1 B3LYP/6-31G** energy profiles for the radical transformations leading from **7** to **11** and **11a** in benzene; **7**, **11** and **11a** are off the scale.

shown in Fig. 1 and Table 1; finally, geometries of the involved transition states are shown in Fig. 2.

For the conversion of **7** into **11** or **11a** (not observed) two possible reaction paths (paths 1 and 2 in Scheme 4) have been investigated. In this mechanism, radical cyclisation or hydrogen translocation from the initially generated 1-(carbamoyl)dichloromethyl radical are assumed to be faster than hydrogen abstraction, as experimentally evidenced in the morphan series.⁷ In path 1, the initial intermediate **R-1** undergoes an intramolecular attack of the dichloromethyl radical onto the olefinic carbon with simultaneous six-membered ring formation, through **TS1**, to give cyclic radical **R-2**. Final reduction of the radical intermediate **R-2** leads to the diastereomeric mixture of methylpiperidones **11**. It is worth noting that the possibility for the radical **R-1** to attack the olefin by its *re*-face and *si*-face results in two transition states, **TS1-re** and **TS1-si**, respectively.

In the reaction path 2, **R-1** suffers an intramolecular hydrogen transfer from the benzylic position to the dichloromethyl group, through **TS2**, leading to benzyl radical **R-3**, which is stabilised by conjugation with the aromatic ring. Intramolecular attack of **R-3** to the olefinic carbon with simultaneous five-membered ring formation through **TS3** gives rise to **R-4**. Subsequent reduction would afford the epimeric mixture of methylpyrrolidines **11a**. As mentioned above for path 1, both **TS3-re** and **TS3-si** may result from the radical attack on both faces of the olefin, giving rise to radicals **R-4-re** and **R-4-si**, respectively.

The conversion of dichloromethyl radical **R-1** into the piperidine radical **R-2-re** has an energy barrier of 12.8 kcal mol⁻¹ (**TS1-re**), while the energy barrier for the transformation into piperidone radical **R-2-si** is 13.4 kcal mol⁻¹ (**TS1-si**) (see Fig. 1 and Table 1).

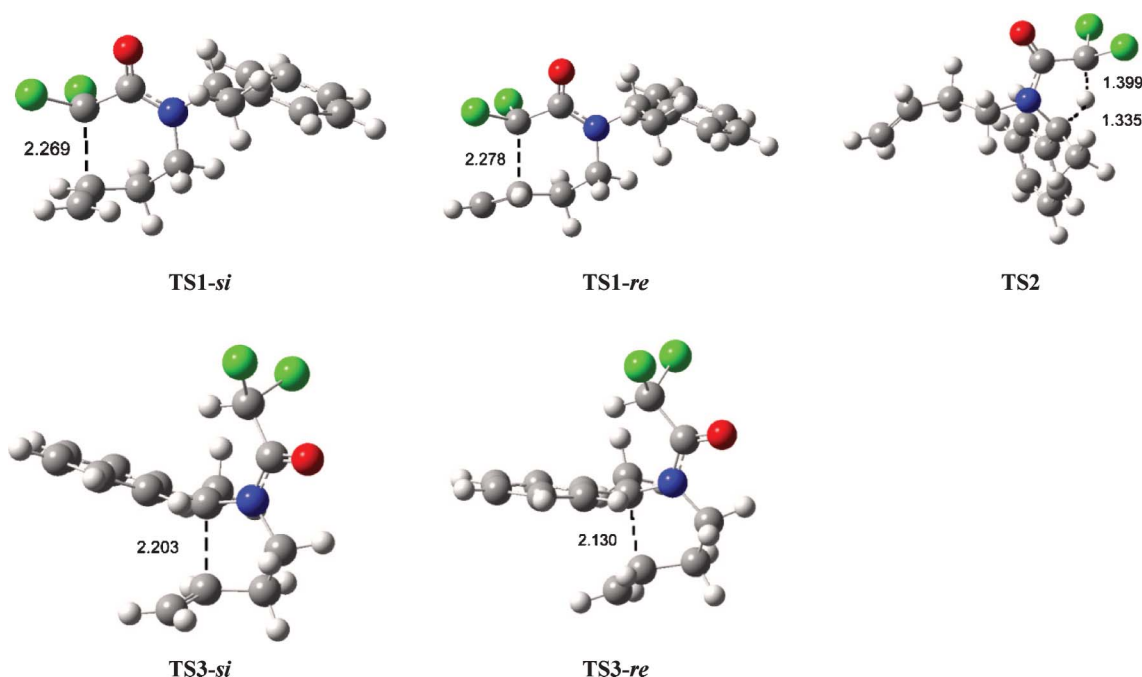
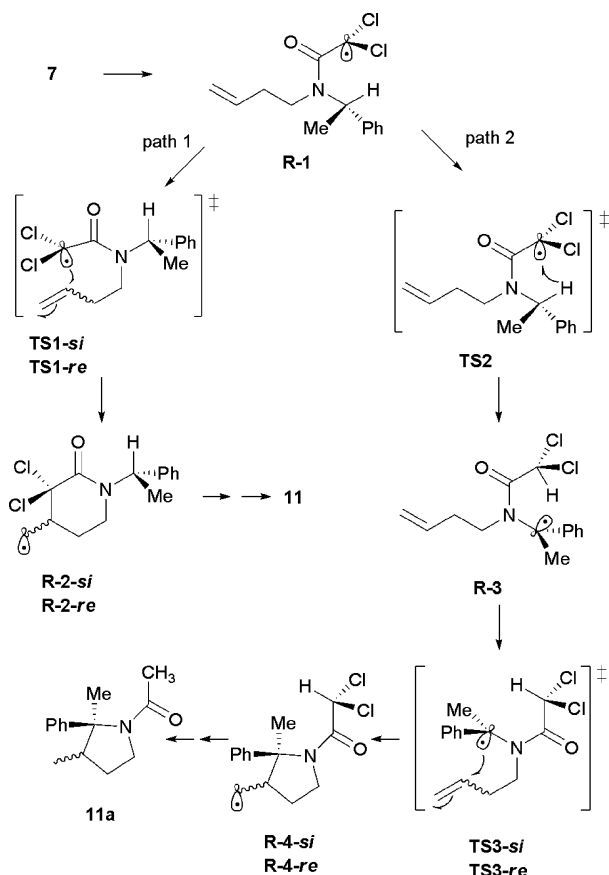


Fig. 2 The transition states for the conversion of **7** into **11** and **11a** through the mechanism postulated in Scheme 4. Bond length values are given in Å.



Scheme 4 The suggested mechanism for the conversion of **7** into **11** and **11a**.

These energy values indicate that the attack of radical **R-1** on the *re*-face of the olefin is, from a kinetic point of view, slightly

favoured. However, this energy difference still allows competition between both pathways in agreement with the observed experimental results. Overall, the conversion of **R-1** into **R-2-re** and **R-2-si** is thermodynamically favoured by 11.9 and 10.7 kcal mol⁻¹, respectively.

On the other hand, the conversion of radical **R-1** into the pyrrolidine radical **R-4** (path 2, Scheme 4) has an energy barrier of 14.5 kcal mol⁻¹ (**TS2**). The initial hydrogen transfer is the rate determining step of the process (**TS2**), being more energetic than the subsequent intramolecular attack of the benzyl radical to the *re*-face or *si*-face of the olefin (**TS3-re** and **TS3-si**, 6.3 and 8.9 kcal mol⁻¹, respectively). Hence, **TS2** (path 2) is 1.7 and 1.1 kcal mol⁻¹, respectively, above **TS1-re** and **TS1-si** (path 1). As a consequence, the methylpyrrolidines **11a** should be minor products in the reaction mixture (*ca.* 3%), and may or may not be observed.

ii) **Conversion of 3b into 4b and 5b.** The mechanism proposed for the transformation of **3b** into **4b** and **5b** (Scheme 5) is based on a theoretical treatment analogous to that described above for the conversion of **7** into **11** and **11a**. The energies of the relevant species are shown in Fig. 3 and Table 2. Fig. 4 shows the geometries of the transition states involved in the proposed mechanism.

In this case, the starting point is the most stable conformer of dichloromethyl radical **R-5**, bearing the acetamide moiety at the equatorial position, that can evolve through paths 1 or 2. Along the former path, **R-5** is first converted into its conformer **R-5a** by rotation of the N–CO bond through transition state **TS4**. Then, **R-5a** changes to the inverted-chair conformation **R-5b**, through **TS5**, in order to make the subsequent attack to the double bond (by **TS6**) feasible. It is worth noting that inversion of the chair conformation prior to the N–CO bond rotation, results in a higher energetic barrier. Reduction of the intermediate **R-6** leads to azabicyclononane **4b**. The radical attack is only possible

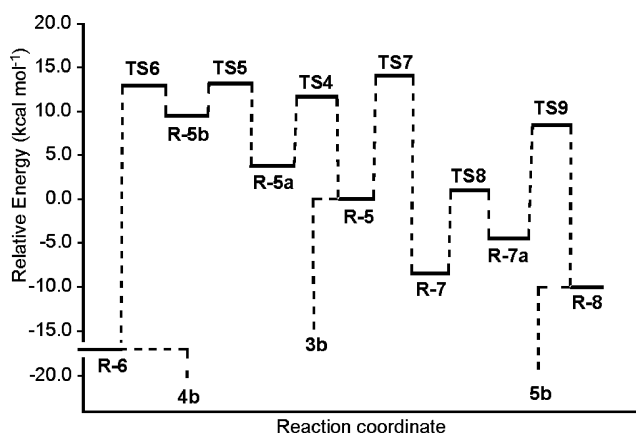


Fig. 3 B3LYP/6-31G** energy profiles for the radical transformations of **3b** leading to **4b** and **5b** in benzene; **3b**, **4b** and **5b** are off the scale.

from the same side of the molecule, due to the conformational restrictions of **TS6**, giving rise to only one diastereoisomer of **4b**.

In path 2, radical **R-5** undergoes an intramolecular hydrogen transfer from the benzylic position to the dichloromethyl group through transition state **TS7**. The stabilised benzyl radical intermediate **R-7** suffers a conformational change of the cyclohexene ring to an inverted-chair, with simultaneous rotation of the C1–N bond (through **TS8**), leading to radical **R-7a**. Finally, **R-7a** undergoes an intramolecular radical addition at the olefinic carbon with simultaneous five-membered ring-formation (through **TS9**), giving rise to **R-8**. Eventually, reduction of this radical affords normorphan **5b**.

Thus, dichloromethyl radical **R-5** is converted into **R-6** through three transition states **TS4**, **TS5** and **TS6** with relative energy values of 11.6, 13.2 and 13.1 kcal mol^{−1}, respectively (see Fig. 3

Table 2 Total (*E*, au) and relative energies (ΔE , kcal mol^{−1}), at the B3LYP/6-31G** level in benzene, of the stationary points for the radical transformations of **3b** into **4b** and **5b**

	<i>E</i>	ΔE
R-5	−1763.124648	0.00
TS4	−1763.106144	11.6
R-5a	−1763.118500	3.9
TS5	−1763.103677	13.2
R-5b	−1763.109453	9.5
TS6	−1763.103828	13.1
R-6	−1763.151660	−17.0
TS7	−1763.102159	14.1
R-7	−1763.137806	−8.3
TS8	−1763.122957	1.1
R-7a	−1763.131537	−4.3
TS9	−1763.111040	8.5
R-8	−1763.140392	−9.9

and Table 2). As **TS5** and **TS6** have similar energetic levels, they are the rate limiting steps. The dichloromethyl radical **R-5**, stabilised by interaction with the benzylic hydrogen, is converted into the less stable radical **R-5a** (+3.9 kcal mol^{−1}). The subsequent conversion of **R-5a** into **R-5b** is clearly a disfavoured step from an energetic point of view (+5.6 kcal mol^{−1}). Remarkably, formation of **R-6** from **R-5b** is thermodynamically favoured. On the other hand, the transformation of **R-5** into **R-8** has an energetic barrier of 14.1 kcal mol^{−1} (**TS7**) that corresponds to the initial hydrogen transfer. This step is more energetic than the subsequent conformational change (**TS8** = 1.1 kcal mol^{−1}) and than the intramolecular attack of the benzyl radical at the olefinic carbon (**TS9** = 8.5 kcal mol^{−1}). The transformation of **R-5** into **R-7** is exothermic (−8.3 kcal mol^{−1}) due to stabilisation of the benzyl radical formed. The conformational change from **R-7** to **R-7a** is again an endothermic step (+4.0 kcal mol^{−1}); however, the radical

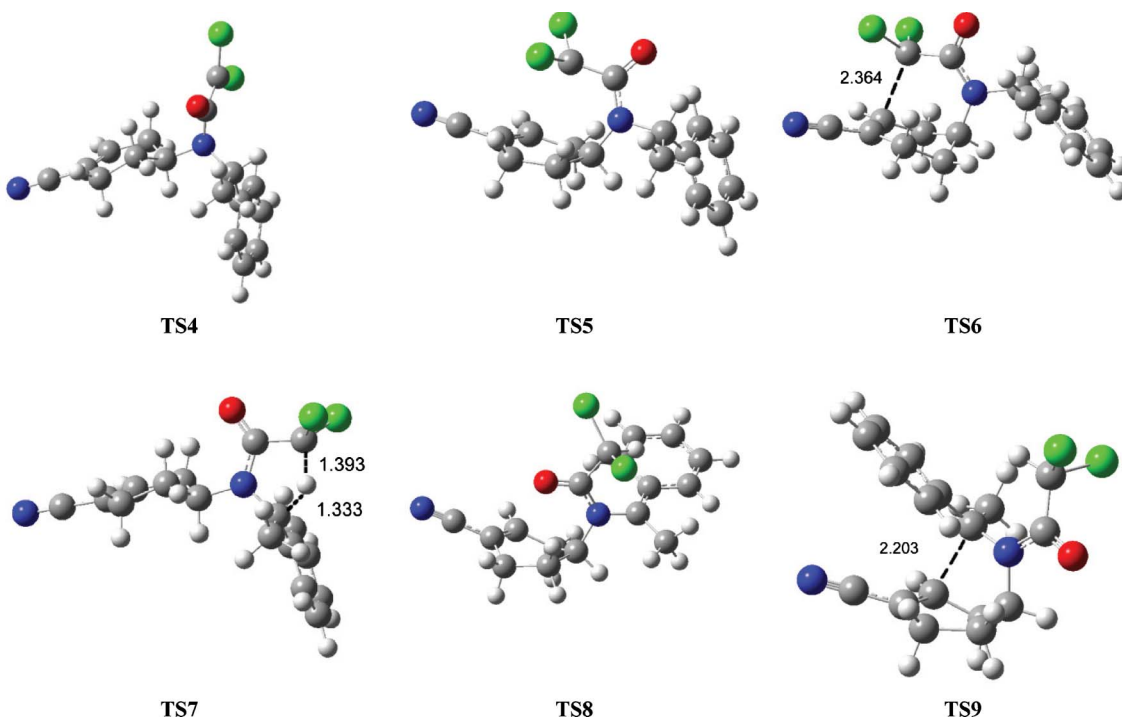
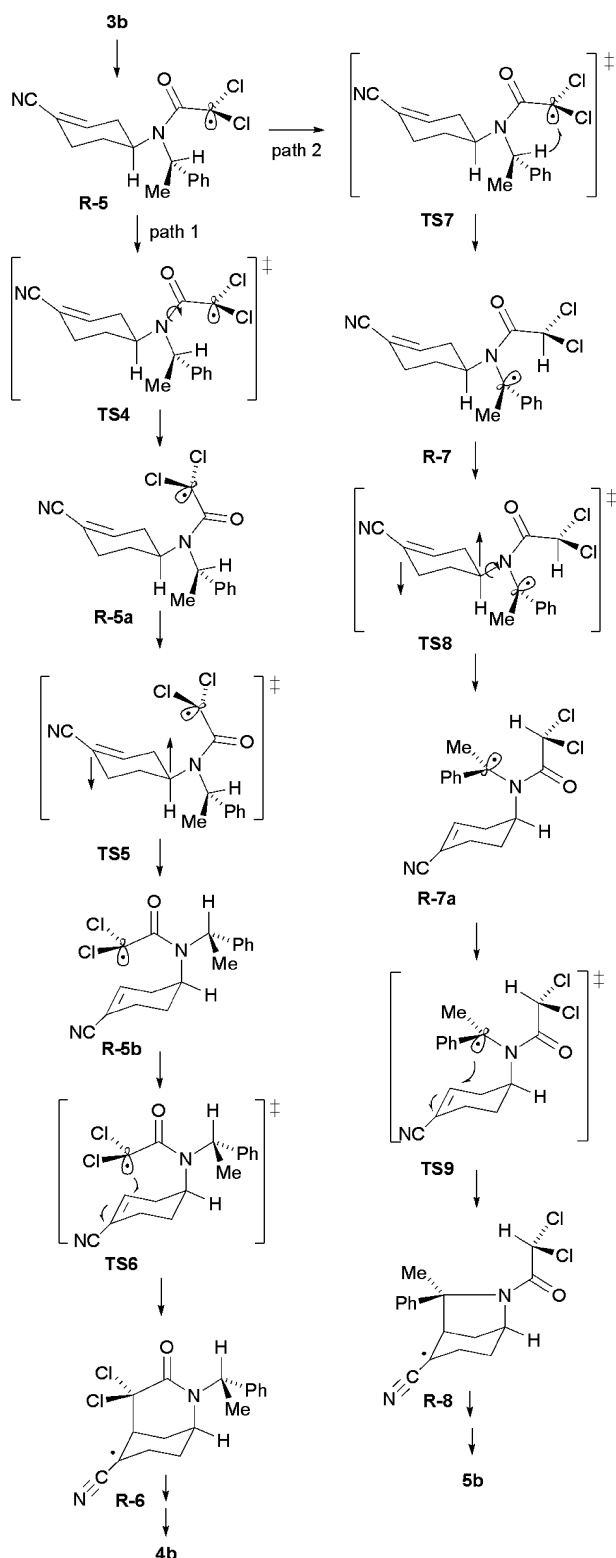


Fig. 4 Transition structures corresponding to the conversion of **3b** into **4b** and **5b**. Bond length values are given in Å.



Scheme 5 The suggested mechanism for the conversion of **3b** into **4b** and **5b**.

attack on the double bond giving rise to the bicyclic radical **R-8** is exothermic ($-5.6 \text{ kcal mol}^{-1}$).

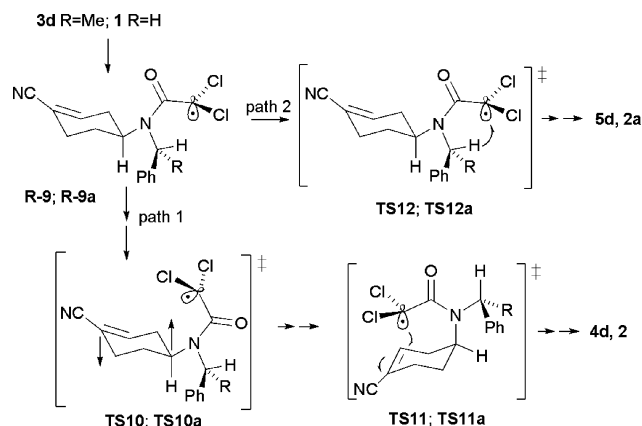
Overall, both proposed pathways are exothermic by $-17.0 \text{ kcal mol}^{-1}$ and $-9.9 \text{ kcal mol}^{-1}$, respectively. When the energetic barriers of both pathways are compared, **TS5/TS6** for

Table 3 Total (E , au) and relative energies (ΔE , kcal mol^{-1}), at the B3LYP/6-31G** level in benzene, of the most relevant transition states for the radical transformations of **3d** and **1** into **4d/5d** and **2/2a**

	E	ΔE
R-9	-1763.117817	0.0
TS10	-1763.095888	13.8
TS11	-1763.096831	13.2
TS12	-1763.094658	14.5
T9a	-1723.802658	0.0
TS10a	-1723.781910	13.0
TS11a	-1763.785349	10.9
TS12a	-1763.777087	16.1

path 1 and **TS7** for path 2, that of the former is $0.9 \text{ kcal mol}^{-1}$ lower. This small difference allows competition between the two pathways, with the formation of azabicyclononane **4b** being slightly favoured over that of normorphane **5b**, in agreement with the experimentally observed results.

iii) Conversion of 3d and 1 into 4d/5d and 2/2a. From the above theoretical calculations, the rate limiting steps for the conversion of **3b** into **4b/5b** are **TS5/TS6** and **TS7**, respectively. Hence, to simplify the theoretical study for the conversion of **3d** into **4d/5d** and **1** into **2/2a** only those transition states have been considered (for clarity, compound **3d** has been depicted as its enantiomer, see Scheme 6). The energies of the relevant species are shown in Table 3. Fig. 5 shows the geometries of the involved transition states.



Scheme 6 A simplified mechanism for the conversion of **3d** and **1** into **4d/5d** and **2/2a**.

Here, **R-9** is the initially formed radical in the transformation of **3d** into **4d** or **5d**. Transition states **TS10** and **TS11** correspond to the energetic barriers for the conformational change for chair inversion and intramolecular radical attack to the olefinic carbon, respectively, along path 1. Likewise, **TS12** is the barrier for the translocation of the benzylic hydrogen to the dichloromethyl moiety leading to **5d** along path 2. The equivalent species for the transformation of trichloroacetamide **1** into the azabicyclononane **2** or normorphane **2a** (not experimentally observed) are **R-9a**, **TS10a**, **TS11a** and **TS12a**.

The energetic barriers for the conversion of **3d** into **4d/5d** are similar to the ones calculated above for the epimer **3b** (see Table 3). Again, **TS10** and **TS11** (path 1) have very similar values ($13.8 \text{ kcal mol}^{-1}$ and $13.2 \text{ kcal mol}^{-1}$, respectively) while **TS12**

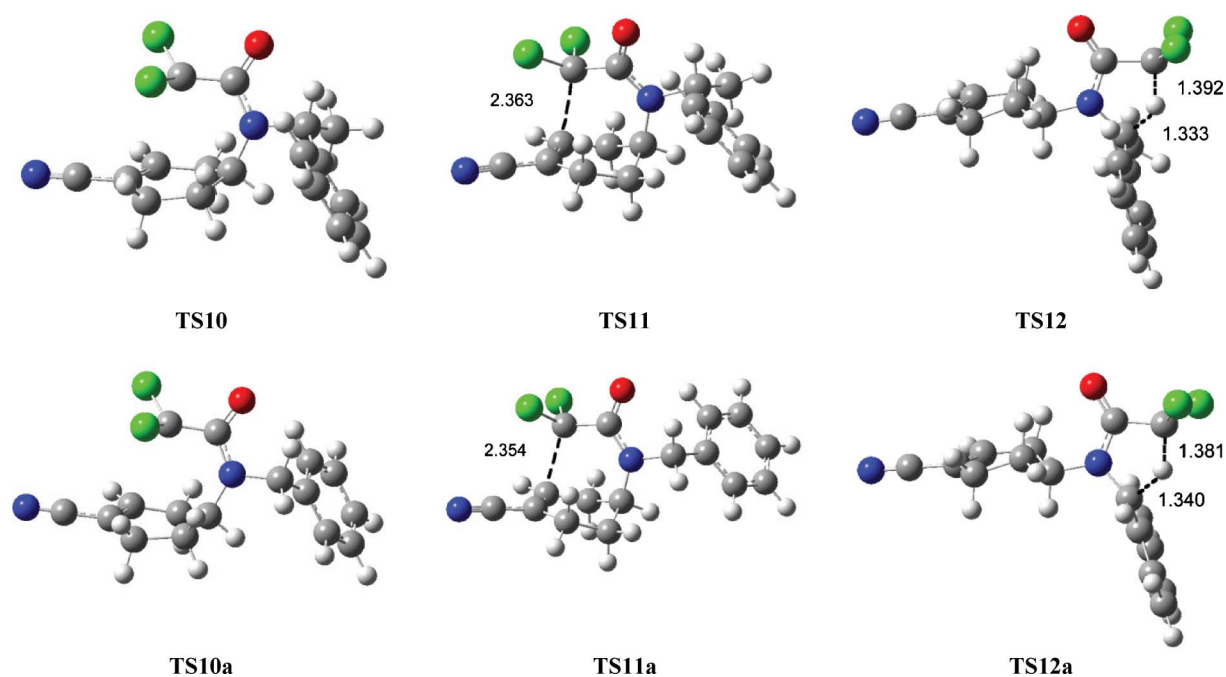


Fig. 5 Transition structures corresponding to the conversion of **3d** and **1** into **4d/5d** and **2/2a**. Bond length values are given in Å.

(path 2) is higher in energy (14.5 kcal mol⁻¹). When the energetic barriers for the two pathways are compared, **TS10** for path 1 and **TS12** for path 2, that of the former is 0.7 kcal mol⁻¹ lower. This difference is slightly smaller than that observed for the isomer **3b** (0.9 kcal mol⁻¹) and supports the experimentally observed trend of increased translocation product **5d**.

Finally, the theoretical calculations are significantly different for trichloroacetamide **1**, which contains a benzyl instead of a 1-phenylethyl group. The energies of the implied transition states in path 1 for conversion of **1** into **2** (**TS10a** and **TS11a**) are lower (13.0 kcal mol⁻¹ and 10.9 kcal mol⁻¹, respectively) than in the case of **TS10** and **TS11**. On the other hand, **TS12a** (the energetic barrier for the conversion of **1** into **2a** through path 2 is now 16.1 kcal mol⁻¹, much higher than **TS12** (14.5 kcal mol⁻¹). This is reasonable, in view of the lower stability of secondary *versus* tertiary benzylic radicals. As a conclusion, the energy barrier for the conversion of **1** into **2** through path 1 is clearly lower by 3.1 kcal mol⁻¹ than for the conversion of **1** into **2a** through path 2. These calculations are in complete agreement with the experimental results, and explain why normorphane **2a** was not observed.

Summary and conclusions

The radical cyclisation of *N*-cyclohexenyl trichloroacetamides using AIBN/TTMSS gives rise to 2-azabicyclo[3.3.1]nonanes with good overall yields. However, when *N*-cyclohexenyl-*N*-(1-phenylethyl) trichloroacetamides are submitted to similar conditions, normorphane derivatives are also isolated. The former are the result of the expected 6-*exo*-trig radical cyclisation, whereas the latter come from a competitive process involving a 1,4-hydrogen transfer, followed by a 5-*exo*-trig cyclisation. When the same experimental conditions were applied to trichloroacetamides bearing an *N*-(1-phenylethyl) substituent and a simple open-

chain alkenyl moiety, the obtained products result only from the cyclisation of the 1-(carbamoyl)dichloromethyl radical onto the double bond. The 1,4-translocation products are not detected. Therefore, it seems that the two structural features are required for the translocation to occur, namely the alkyl benzyl moiety and the cyclohexene ring.

Theoretical DFT calculations have been performed to explain the formation of products resulting from cyclisation of the 1-(carbamoyl)dichloromethyl radical onto the double bond (path 1) and/or the products arising from translocation of the benzylic hydrogen to the dichloromethyl moiety followed by a cyclisation (path 2). The relative energy barriers for the involved processes are in good agreement with the experimental results.

Experimental Section

General

All reactions were carried out under an argon atmosphere with dry, freshly distilled solvents under anhydrous conditions. Analytical thin-layer chromatography was performed on SiO₂ (Merck silica gel 60 F₂₅₄), and the spots were located with 1% aqueous KMnO₄ or 2% ethanolic anisaldehyde. Chromatography refers to flash chromatography and was carried out on SiO₂ (SDS silica gel 60 ACC, 35–75 μm, 230–240 mesh ASTM). The drying of organic extracts during work-up of the reactions was performed over anhydrous MgSO₄, except where stated otherwise. NMR spectra were recorded in CDCl₃ on a Varian Gemini 300 or Varian VNMRs 400. Chemical shifts of ¹H and ¹³C NMR spectra are reported in ppm downfield (δ) from Me₄Si.

N-[(*S*)-1-phenylethyl]-*N*-(2-propenyl)-2,2,2-trichloroacetamide **6**

To a solution of *N*-[(*S*)-1-phenylethyl]allylamine¹² (470 mg, 2.92 mmol) in CH₂Cl₂ (15 mL) was added triethylamine (0.81 mL,

5.84 mmol) and the solution was cooled to 0 °C. Trichloroacetyl chloride (0.49 mL, 4.38 mmol) in CH₂Cl₂ (1.5 mL) was added and the resulting mixture was heated under reflux for 24 h. The reaction mixture was concentrated, and the resulting residue was dissolved in CH₂Cl₂, washed with 1 N aqueous HCl, and saturated aqueous Na₂CO₃. The organic layer was dried, concentrated, and purified by chromatography (10% EtOAc–hexane) to give **6** (643 mg, 72%) as a yellow oil: IR (NaCl) 1668 (CO); ¹H NMR (300 MHz, 50 °C) 1.74 (d, *J* = 7 Hz, 3 H), 3.51 and 4.12 (2 br s, 2 H), 5.04–5.14 (m, 2 H), 5.74–5.90 (m, 2 H), 7.20–7.40 (m, 5 H); ¹³C NMR (75 MHz, DEPT) 17.7 (CH₃), 48.6 (C-1), 56.8 (CH), 93.4 (CCl₃), 117.1 (C-3), 126.5, 127.5, 128.4 (C-*o*, C-*m*, C-*p*), 132.5 (C-2), 138.8 (C-*ipso*), 159.9 (CO). Anal. calcd for C₁₃H₁₄Cl₃NO: C, 50.92; H, 4.60; N, 4.57. Found: C, 50.77; H, 4.65; N, 4.45.

N-(2-butenyl)-*N*-[(*S*)-1-phenylethyl]-2,2,2-trichloroacetamide **7**

Similarly, from *N*-(2-butenyl)-*N*-[(*S*)-1-phenylethyl]amine¹³ (284 mg, 1.63 mmol) and after chromatography (hexane/EtOAc, 9:1) trichloroacetamide **7** (489 mg, 94%) was isolated as a yellow oil. All spectroscopic data were in accordance with those previously reported.¹⁰ IR (NaCl): 1670; ¹H NMR (300 MHz) 1.60 (d, *J* = 7 Hz, 3H, CH₃), 2.22 (m, 2H, CH₂), 2.74 and 3.25 (2 m, 1H each, CH₂), 4.82 (m, 2H, CH₂), 5.48 (m, 1H, CH), 5.73 (m, 1H, CH), 7.20–7.40 (m, 5H); ¹³C NMR (75 MHz, DEPT) 17.9 (CH₃), 32.3 (C-2), 46.4 (C-1), 56.8 (CH), 94.2 (CCl₃), 117.0 (C-4), 127.0, 127.7, 128.6 (C-*o*, C-*m*, C-*p*), 135.2 (C-3), 139.0 (C-*ipso*), 160.2 (CO). HRMS (ESI-TOF): calcd for C₁₄H₁₇Cl₃NO 320.0370 (M⁺ + 1). Found 320.0374.

N-(3-oxopropyl)-*N*-[(*S*)-1-phenylethyl]-2,2,2-trichloroacetamide **8**

A stirred solution of **7** (1.88 g, 5.87 mmol) in CH₂Cl₂ (19.4 mL) at –78 °C was charged with a constant stream of ozone. After 15 min, the solution was purged with Ar until it was clear and then Me₂S (11.6 mL, 158 mmol) was added. The reaction mixture was left at rt for 48 h. It was diluted with CH₂Cl₂ (50 mL), washed with brine, dried and concentrated. Purification of the residue by chromatography (20% EtOAc–hexane) gave aldehyde **8** (1.37 g, 73%) as a clear oil: IR (NaCl): 1670, 1724; ¹H NMR (400 MHz) 1.74 (d, *J* = 6.9 Hz, 3H, CH₃), 2.50–2.76 (m, 2H, CH₂), 3.24–3.40 (m, 1H, NCH), 3.48–3.64 (m, 1H, NCH), 5.82–5.94 (q, *J* = 6.9 Hz, 1H, CH), 7.30–7.50 (m, 5H, ArH), 9.63 (s, 1H, CHO); ¹³C NMR (100 MHz, DEPT) 17.3 (CH₃), 39.9 (CH₂), 42.3 (NCH₂), 56.8 (CH), 126.8, 128.0 and 128.7 (C-*o*, C-*m*, C-*p*), 138.3 (C-*ipso*), 160.4 (CO), 199.5 (CO). Anal. calcd for C₁₃H₁₄Cl₃NO₂: C, 48.40; H, 4.37; N, 4.34. Found: C, 48.27; H, 4.34; N, 4.27.

N-(3-acetoxyprop-2-enyl)-*N*-[(*S*)-1-phenylethyl]-2,2,2-trichloroacetamide **9**

To a solution of *p*-toluenesulfonic acid monohydrate (6 mg, 0.032 mmol) in isopropenyl acetate (1.5 mL) warmed at reflux temperature was added a solution of aldehyde **8** (103 mg, 0.32 mmol) in isopropenyl acetate (3 mL) and the mixture was stirred for 24 h. To the cooled reaction mixture was added Et₂O (10 mL) and the solution was washed with 5% aqueous NaHCO₃ and H₂O. The aqueous extracts were extracted with EtOAc, and the combined organic layers were dried, and concentrated. Purification of the residue by chromatography (Florisil™, 5%

EtOAc–hexane) gave enol acetate **9** (80 mg, 68%) as a yellow oil and as an *E*:*Z* isomeric mixture (6:4 according to ¹H-NMR): IR (NaCl) 1760, 1674; ¹H NMR (400 MHz) 1.74 (br s, 3H, CH₃), 2.05, 2.10 (2 s, 3H, CH₃CO), 3.40–3.55 and 3.85–4.00 (2 m, 1.2H, *E* isomer, CH₂N), 3.60–3.75 and 4.00–4.10 (2 m, 0.8H, *Z* isomer, CH₂N), 5.00 (m, 0.4H, *Z* isomer, CH=), 5.40–5.50 (m, 0.6H, *E* isomer, CH=), 5.80–6.00 (m, 1H, CH), 7.01 (dt, *J* = 6.3, 1.2 Hz, 0.4H, *Z* isomer, OCH=), 7.08 (dm, *J* = 12.9 Hz, 0.6H, *E* isomer, OCH=), 7.20–7.40 (m, 5H, ArH); ¹³C NMR (100 MHz, DEPT) 17.4, 17.9 (CH₃), 20.6 (CH₃CO), 41.1 (CH₂N, *Z* isomer), 44.0 (CH₂N, *E* isomer), 56.9 (CH), 108.4 (CH=, *Z* isomer), 108.8 (CH=, *E* isomer), 126.9, 127.7, 127.8, 128.6 (C-*o*, C-*m*, C-*p*), 135.1 (=CHO), 138.6, 139.0 (=CHO), 160.1 (CO), 167.1, 167.5 (CO). Anal. calcd for C₁₅H₁₆Cl₃NO₃: C, 49.41; H, 4.42; N, 3.84. Found: C, 49.24; H, 4.48; N, 3.69.

(4*R*)- and (4*S*)-4-methyl-1-[(*S*)-1-phenylethyl]pyrrolidin-2-one **10**

A suspension of **6** (201 mg, 0.66 mmol) and AIBN (115 mg, 0.70 mmol) in benzene (6 mL) was heated to reflux. Then, TTMSS (0.71 mL, 2.30 mmol) was added dropwise and the reaction mixture was stirred at this temperature for 2 h and concentrated. Purification of the residue by chromatography (CH₂Cl₂) gave **10** (106 mg, 80%) as a yellow oil and as an epimeric mixture (1:1 ratio by ¹H-RMN). All spectroscopic data were in accordance with those previously reported.¹⁴ IR (NaCl) 1670; ¹H NMR (300 MHz) 0.97 and 1.10 (2d, *J* = 7 Hz, 3H, CH₃), 1.50 (d, *J* = 7 Hz, 3H, CH₃), 2.00 (dd, *J* = 16.5, 6.3 Hz, 0.5 H), 2.05 (dd, *J* = 16.5, 7.2 Hz, 0.5H) 2.20–2.40 (m, 1H), 2.50–2.60 (m, 1.5H), 2.85 (dd, *J* = 9.4 and 6.4 Hz, 0.5H), 3.10 (dd, *J* = 9.4 and 7.6 Hz, 0.5H), 3.40 (dd, *J* = 9.3 and 7.5 Hz, 0.5H), 5.50 (q, *J* = 7 Hz, CH), 7.25–7.40 (m, 5H); ¹³C NMR (75 MHz, DEPT) 16.6 (CH₃), 20.0 (CH₃), 26.8, 27.1 (C-4), 40.3 (C-3), 49.2 (CH), 49.9, 50.3 (C-5), 127.5, 127.9, 128.9 (C-*o*, C-*m*, C-*p*), 140.8 (C-*ipso*), 174.4 (CO). HRMS (ESI-TOF): calcd for C₁₃H₁₈NO 204.1383 (M⁺ + 1). Found 204.1388.

(4*R*)- and (4*S*)-1-[(*S*)-1-phenylethyl]-4-methylpiperidin-2-one **11**

Similarly, trichloroacetamide **7** (290 mg, 0.91 mmol) in benzene (8.7 mL) was treated with AIBN (164 mg, 1.00 mmol) and TTMSS (0.98 mL, 3.17 mmol), and the crude material was purified by chromatography (EtOAc) to give **6** (105 mg, 53%) as a yellow oil and as an epimeric mixture (1:1 ratio by ¹H-RMN): IR (NaCl) 1634; ¹H NMR (400 MHz) 0.95, 0.97 (2 d, *J* = 2.4 Hz, 3H, CH₃), 1.24 (dtd, *J* = 13.6, 10.4, 5.6 Hz, 0.5 H, H-5_{ax}), 1.49 and 1.50 (2 d, *J* = 6.9 Hz, 3H, CH₃), 1.75 (dm, *J* = 13.2 Hz, 0.5H, H-5_{eq}), 1.80–2.00 (m, 1H, H-4), 2.06 (dd, *J* = 17.2, 3.6 Hz, 0.5H, H-3), 2.08 (dd, *J* = 17.2, 4.4 Hz, 0.5H, H-3), 2.56 (td, *J* = 5.2, 2 Hz, 0.5H, H-3), 2.61 (td, *J* = 5.3, 2 Hz, 0.5H, H-3), 2.66 (ddd, *J* = 12.5, 10.5, 4.6 Hz, 0.5H, H-6_{ax}), 2.86 (ddd, *J* = 12.1, 4.8, 3.4 Hz, 0.5H, H-6_{eq}), 3.07–3.16 (m, 1H, H-6), 6.14 (q, *J* = 7 Hz, 1H, CH), 7.20–7.40 (m, 5H, ArH); ¹³C NMR (100 MHz, DEPT) 15.0, 15.3 (CH₃), 20.8, 21.1 (CH₃), 27.3, 27.8 (C-4), 30.7, 30.8 (C-5), 40.2, 40.4, 40.5, 40.6 (C-3 and C-6), 49.3, 49.4 (CH), 126.9, 127.0, 127.3, 128.2 (C-*o*, C-*m*, C-*p*), 140.0, 140.5 (C-*ipso*), 169.1, 169.2 (C-2). Anal. calcd for C₁₄H₁₉NO: C, 77.38; H, 8.81; N, 6.45. Found: C, 77.21; H, 8.84; N, 6.40.

(4R)- and (4S)-4-acetoxymethyl-1-[(S)-1-phenylethyl]pyrrolidin-2-one 12

Following the above procedure for the cyclization of **6** to **10**, from trichloroacetamide **9** (282 mg, 0.77 mmol) with a 3 h reaction time, pyrrolidone **12a** (78 mg) and its epimer **12b** (79 mg) were obtained after chromatography (EtOAc) as yellow oils (78% overall yield). **12a**: IR (NaCl) 1741, 1684; ¹H NMR (400 MHz) 1.52 (d, *J* = 6.8 Hz, 3H, CH₃), 2.05 (s, 3H, CH₃CO), 2.26 (dd, *J* = 20.4, 10 Hz, 1H, H-3), 2.58 (dd, *J* = 19.8, 8.4 Hz, 1H, H-3), 2.56–2.62 (m, 1H, H-4), 3.09 (d, *J* = 6 Hz, 2H, H-5), 4.02 (dd, *J* = 11.4, 6.8 Hz, 1H, CHO), 4.08 (dd, *J* = 11.2, 5.6 Hz, 1H, CHO), 5.50 (q, *J* = 7.2 Hz, 1H, CH), 7.20–7.40 (m, 5H, ArH); ¹³C NMR (100 MHz, DEPT) 16.0 (CH₃), 20.7 (CH₃CO), 30.4 (C-4), 34.4 (C-3), 44.8 (C-5), 48.9 (CH), 65.9 (CH₂O), 127.0, 127.5 and 128.5 (C-*o*, C-*m*, C-*p*), 139.8 (C-*ipso*), 170.8 (CO), 172.7 (CO). Anal. calcd for C₁₅H₁₉NO₃·1/10 H₂O: C, 68.47; H, 7.35; N, 5.32. Found: C, 68.30; H, 7.55; N, 5.37. **12b**: IR (NaCl): 1740, 1683; ¹H NMR (400 MHz) 1.53 (d, *J* = 7.2 Hz, 3H, CH₃), 1.97 (s, 3H, COCH₃), 2.23 (ddd, *J* = 19.6, 10, 4.2 Hz, 1H, H-3), 2.53–2.67 (m, 2H, H-3, H-4), 2.74 (dd, *J* = 10, 4.8 Hz, 1H, H-5), 3.45 (dd, *J* = 10, 7.6 Hz, 1H, H-5), 3.87 (dd, *J* = 10.8, 6.8 Hz, 1H, CHO), 3.94 (dd, *J* = 10.6, 6 Hz, 1H, CHO), 5.50 (q, *J* = 7.2 Hz, 1H, CH), 7.20–7.40 (m, 5H, ArH); ¹³C NMR (100 MHz, DEPT) 16.0 (CH₃), 20.6 (CH₃CO), 30.1 (C-4), 34.5 (C-3), 44.9 (C-5), 49.0 (CH), 65.8 (CH₂O), 127.0, 127.6 and 128.5 (C-*o*, C-*m*, C-*p*), 139.8 (C-*ipso*), 170.7 (CO), 172.8 (CO). Anal. calcd for C₁₅H₁₉NO₃·1/2 H₂O: C, 66.64; H, 7.46; N, 5.18. Found: C, 66.64; H, 7.37; N, 5.18.

Computational methods

All calculations were carried out with the Gaussian 03 suite of programs.¹⁵ Density functional theory¹⁶ calculations (DFT) have been carried out using the B3LYP¹⁷ exchange–correlation functionals, together with the standard 6-31G** basis set.¹⁸ The stationary points were characterized by frequency calculations in order to verify that minima and transition structures have zero and one imaginary frequency, respectively. The inclusion of solvent effects has been considered by using a relatively simple self-consistent reaction field (SCRF) method¹⁹ based on the polarizable continuum model (PCM) of Tomasi's group.²⁰ We have used benzene as the solvent. Gaussian treats H atoms as part of a fragment (OH, CH, SH *etc.*) when creating cavities in the PCM model. In some cases (*e.g.* heavy atom–H bond is elongated), cavity building fails. For this reason, we have used the cavity model that also assigns spheres to hydrogens (radii = uff).

Acknowledgements

This research was supported by the Ministry of Education and Science (Spain)–FEDER through projects CTQ2007-61338/BQU, CTQ2009-11027/BQU and CTQ2009-13699 and Universidad Politecnica de Valencia (2005-PPI-06-05).

Notes and references

- (a) A. J. Clark, *Chem. Soc. Rev.*, 2002, **31**, 1; (b) M. Pattarozzi, F. Roncaglia, V. Giangiordano, P. Davoli, F. Prati and F. Ghelfi, *Synthesis*, 2010, 694; (c) Y. Motoyama, K. Kamo, A. Yuasa and H. Nagashima, *Chem. Commun.*, 2010, **46**, 2256.
- (a) B. A. Seigal, C. Fajardo and M. L. Snapper, *J. Am. Chem. Soc.*, 2005, **127**, 16329; (b) C. D. Edlin, J. Faulkner and P. Quayle, *Tetrahedron Lett.*, 2006, **47**, 1145; (c) F. I. McGonagle, L. Brown, A. Cooke and A. Sutherland, *Org. Biomol. Chem.*, 2010, **8**, 3418.
- J. Quirante, C. Escolano, A. Merino and J. Bonjoch, *J. Org. Chem.*, 1998, **63**, 968.
- X. Vila, J. Quirante, L. Paloma and J. Bonjoch, *Tetrahedron Lett.*, 2004, **45**, 4661.
- (a) J. Quirante, C. Escolano, M. Massot and J. Bonjoch, *Tetrahedron*, 1997, **53**, 1391; (b) J. Quirante, C. Escolano, F. Diaba and J. Bonjoch, *Heterocycles*, 1999, **50**, 731; (c) J. Quirante, C. Escolano, F. Diaba and J. Bonjoch, *J. Chem. Soc., Perkin Trans. 1*, 1999, 1157.
- J. Quirante, M. Torra, F. Diaba, C. Escolano and J. Bonjoch, *Tetrahedron: Asymmetry*, 1999, **10**, 2399.
- J. Quirante, F. Diaba, X. Vila, J. Bonjoch, E. Lago and E. Molins, *C. R. Acad. Sci. Paris*, 2001, **4**, 513.
- (a) X. L. Huang and J. J. Dannenberg, *J. Org. Chem.*, 1991, **56**, 5421; (b) M. Gulea, J. M. López-Romero, L. Fensterbank and M. Malacria, *Org. Lett.*, 2000, **2**, 2591; (c) J. Cassayre and S. Z. Zard, *J. Organomet. Chem.*, 2001, **624**, 316.
- For radical cyclizations involving *N*-(α -methylbenzyl) substituted compounds, see: (a) B. Cardillo, R. Galeazzi, G. Mobbili, M. Orena and M. Rossetti, *Heterocycles*, 1994, **38**, 2663; (b) H. Ishibashi, C. Kameoka, K. Kodama and M. Ikeda, *Tetrahedron*, 1996, **52**, 489; (c) H. Ishibashi, Y. Fuke, T. Yamashita and M. Ikeda, *Tetrahedron: Asymmetry*, 1996, **7**, 2531; (d) H. Ishibashi, K. Kodama, C. Kameoka, H. Kawanami and M. Ikeda, *Tetrahedron*, 1996, **52**, 1386; (e) H. Ishibashi, C. Kameoka, K. Kodama, H. Kawanami, M. Humada and M. Okeda, *Tetrahedron*, 1997, **53**, 9611; (f) M. Ikeda, S. Ohtani, T. Sato and H. Ishibashi, *Synthesis*, 1998, 1803.
- A. J. Clark, F. De Campo, R. J. Deeth, R. P. Filik, S. Gatard, N. A. Hunt, D. Lastécouères, G. H. Thomas, J.-B. Verlhac and H. Wongtap, *J. Chem. Soc., Perkin Trans. 1*, 2000, 671.
- R. I. Duclos Jr. and A. Makriyannis, *J. Org. Chem.*, 1992, **57**, 6156.
- (a) G. Cardillo, M. Orena, M. Penna, S. Sandri and C. Tomasini, *Tetrahedron*, 1991, **47**, 2263; (b) B. Cardillo, R. Galeazzi, G. Mobbili, M. Orena and M. Rossetti, *Tetrahedron: Asymmetry*, 1996, **7**, 3573; (c) M. Yus, F. Foubelo and L. R. Falvello, *Tetrahedron: Asymmetry*, 1995, **6**, 2081; (d) V. Rodríguez, M. Sánchez, L. Quintero and F. Sartillo-Piscil, *Tetrahedron*, 2004, **60**, 10809.
- P. Karoyan and G. Chassaing, *Tetrahedron: Asymmetry*, 1997, **8**, 2025.
- For alternative radical procedures leading to **10** and their analytical data, see: (a) M. Ikeda, H. Teranishi, K. Nozaki and H. Ishibashi, *J. Chem. Soc., Perkin Trans. 1*, 1998, 1691; (b) B. Cardillo, R. Galeazzi, G. Mobbili, M. Orena and M. Rossetti, *Heterocycles*, 1994, **38**, 2663.
- M. J. Frisch, G. W. Trucks, H. B. Schlegel, G. E. Scuseria, M. A. Robb, J. R. Cheeseman, J. A. Montgomery Jr., T. Vreven, K. N. Kudin, J. C. Burant, J. M. Millam, S. S. Iyengar, J. Tomasi, V. Barone, B. Mennucci, M. Cossi, G. Scalmani, N. Rega, G. A. Petersson, H. Nakatsuji, M. Hada, M. Ehara, K. Toyota, R. Fukuda, J. Hasegawa, M. Ishida, T. Nakajima, Y. Honda, O. Kitao, O. Nakai, M. Klene, X. Li, J. E. Knox, H. P. Hratchian, J. B. Cross, C. Adamo, J. Jaramillo, R. Gomperts, R. E. Stratmann, O. Yazyev, A. J. Austin, R. Cammi, C. Pomelli, J. W. Ochterski, P. Y. Ayala, K. Morokuma, G. A. Voth, P. Salvador, J. J. Dannenberg, V. G. Zakrzewski, S. Dapprich, A. D. Daniels, M. C. Strain, O. Farkas, D. K. Malick, A. D. Rabuck, K. Raghavachari, J. B. Foresman, J. V. Ortiz, Q. Cui, A. G. Baboul, S. Clifford, J. Cioslowski, B. B. Stefanov, G. Liu, A. Liashenko, P. Piskorz, I. Komaromi, R. L. Martin, D. J. Fox, T. Keith, M. A. Al-Laham, K. N. Peng, A. Nanayakkara, M. Challacombe, P. M. W. Gill, B. Johnson, W. Chen, M. W. Wong, C. Gonzalez and J. A. Pople, *Gaussian 03, Revision C. 02*, Gaussian, Inc., Wallingford CT, 2004.
- (a) R. G. Parr and W. Yang, *Density Functional Theory of Atoms and Molecules*, Oxford University Press, New York, 1989; (b) T. Ziegler, *Chem. Rev.*, 1991, **91**, 651.
- (a) A. D. Becke, *J. Chem. Phys.*, 1993, **98**, 5648; (b) C. Lee, W. Yang and R. G. Parr, *Phys. Rev. B*, 1988, **37**, 785.
- W. J. Hehre, L. Radom, P. V. R. Schleyer and J. A. Pople, *Ab initio Molecular Orbital Theory*, Wiley, New York, 1986.
- (a) J. Tomasi and M. Persico, *Chem. Rev.*, 1994, **94**, 2027; (b) B. Y. Simkin and I. Sheikhet, *Quantum Chemical and Statistical Theory of Solutions – A Computational Approach*, Ellis Horwood, London, 1995.
- (a) E. Cancès, B. Mennucci and J. Tomasi, *J. Chem. Phys.*, 1997, **107**, 3032; (b) M. Cossi, V. Barone, R. Cammi and J. Tomasi, *Chem. Phys. Lett.*, 1996, **255**, 327; (c) V. Barone, M. Cossi and J. Tomasi, *J. Comput. Chem.*, 1998, **19**, 404.